Functional Properties and Microstructure Development of Micro-Nano Fe/MgO Composite

R. Bureš[a,*], M. Fáberová[a], Z. Birčáková[a], P. Kollár[b], J. Füzer[b], M. Jakubčin[b] and P. Slovenský[b]

[a]Institute of Materials Research, Slovak Academy of Sciences, Watsonova 47, 040 01 Košice, Slovak Republic
[b]Institute of Physics, Faculty of Science, Pavol Jozef Šafárik University in Košice, Park Angelinum 9, 041 54 Košice, Slovak Republic

(Received January 23, 2019; revised version January 13, 2020; in final form January 23, 2020)

Micro-nano soft magnetic composite Fe/xMgO was prepared by press and sinter method. The microstructure and functional properties were investigated in dependence on particle size of MgO, as well as on MgO content ratio. Changes of electrical and magnetic properties were clarified on the background of the microstructure development. Particle size of the dielectric MgO phase significantly influenced the densification process, as well as the quality of insulation of each Fe particle from the others, hence the magnetic properties of composite. Significant influence of MgO particle size was observed at frequency of 1 MHz. Value of real part of complex permeability increased with increasing MgO particle size in this order: 10 nm, 1000 nm and the highest value was achieved in Fe/3MgO with 30 nm MgO particles.

DOI: 10.12693/APhysPolA.137.283
PACS/topics: 81.05.–t, 75.50.–y, 62.20.–x

1. Introduction

Relatively new and remarkable kind of soft magnetic materials named soft magnetic composites (SMCs) consists of small ferromagnetic particles electrically insulated from each other. They provide some advantages in comparison with traditional materials (electrical steels or soft magnetic ferrites), as the three-dimensional isotropic physical properties, lower total energy losses at medium to higher frequencies due to lower classical eddy current losses, relatively high saturation induction and the near net shape powder metallurgy fabrication process beneficial from the economical, as well as ecological view [1–4]. SMCs find increasing application potential as cores for transformers, electromotors, generators, electromagnetic circuits, sensors, actuation devices, or induction coils. Each application often requires specific material properties, which can be tuned in wide ranges by the composition of SMC and technological process parameters [1–4].

The most used ferromagnetic component for SMC is the iron powder mainly because of the low cost and high saturation induction. As insulators the inorganic (phosphates, oxides) or the organic (thermoplastics, thermosets) materials are used. Parameters of the heat treatment, relieving internal stresses induced during the compaction of insulated ferromagnetic powder particles, depend on the chosen materials [2, 3].

The quality of insulation of ferromagnetic particles is essential, because of its significant influence on the resulting properties of composite, namely the better the insulation, the lower the classical eddy current losses as these currents are closed within the particles [3, 4]. On the other hand, the negative effect of the SMC structure is the formation of inner demagnetizing fields coming from the surface magnetic poles on insulated ferromagnetic particles [4–6], lowering the magnetic permeability of SMC.

SMC structure observed at the cross-section is based on ferromagnetic micro-islands surrounded by dielectric network. From the viewpoint of the permeability it is desired to achieve thickness of the network as thin as possible. In case of resistivity, the network thickness is limited by effectiveness of the electric insulation. Composites with specific 3D inhomogeneous microstructure based on hierarchic micro–nano structural constituents can be exploited to improve mechanical properties. SMC can be defined as 3D continuous dielectric reinforcement-rich phase with isolated ferromagnetic phase, only the reinforcement-rich phase is continuous to form a grain boundary-like network [7].

The aim of this work was to investigate the powder hierarchic micro–nano composite based on ferromagnetic micro-particles and dielectric nanoparticles, focusing on clarification of the evolution of microstructure and functional properties of pressed and sintered powder composite.

2. Experimental materials and methods

Pure iron powder ASC100.29 (median particle size of 100 μm) supplied by Höganäs AB Sweden was used as primary ferromagnetic component of the composite. Secondary component was magnesium oxide powder. MgO particle size was 10, 30, and 1000 nm with narrow particle size distribution. Fe and MgO powders were dry

*corresponding author; e-mail: rbures@saske.sk

mixed using Resonant acoustic mixer LabRAM. Fe microparticles were covered by smaller MgO nanoparticles, Fe/MgO mixture was shaped by uniaxial die, pressing to the shape of cylinder with diameter of 10 mm and height of 3 mm, prism of size $4 \times 5 \times 20$ mm^3 and ring sample with outer diameter of 24 mm, inner diameter of 18 mm and height of 3 mm. Green compact pressed at pressure of 600 MPa was sintered at 600 °C in dry air atmosphere for 60 min in chamber muffle furnace.

The Fe/MgO composites were prepared with content of 1, 2, 3, 5, 7, and 10 wt% MgO. Microstructure was investigated by light and electron microscopy using LM Nikon LVDia and SEM Jeol JSM 7000F. Resistivity was measured using 4 point probe method by Mitsubishi Loresta AX. Coercive force meter LINKJOIN ATS-320 was used for the measurement of the coercive field of composites at 30 kA/m in an open magnetic circuit. Real part of complex permeability was measured at the frequencies 1 kHz and 1 MHz by impedance spectroscopy using an impedance analyzer HP 4194A with the contact electrodes in two-terminal connection configuration.

3. Results and discussion

3.1. Density

Relative density of the prepared composites depends on MgO particle size as it is documented in Fig. 1. Small addition of MgO up to 2 wt% slightly increases relative density of green compacts. Higher content of MgO above 5 wt% decreases green density. 10 nm MgO nanoparticles influence the relative density significantly less than MgO particles size of 30 nm. 1000 nm MgO particles have the most negative influence on relative green density of the composite. Sintering does not lead to significant increase of relative density of the composite, because creation of Fe–Fe sintering necks is suppressed. Sintered density of the composite based on 1000 nm MgO particles is slightly higher in comparison to composite based on 30 nm particles. The highest is the sintered density of the composite based on 10 nm MgO particles. This fact indicates partial formation of Fe–Fe interparticle connections during sintering of Fe/xMgO based on MgO particles size of 10 nm.

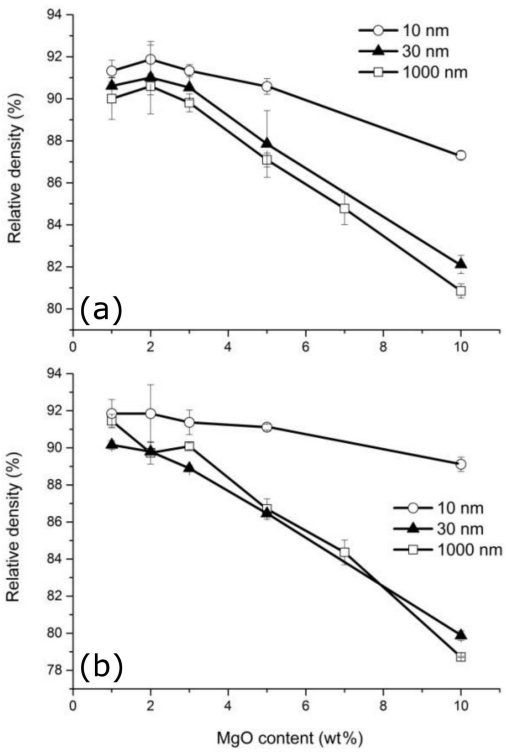

Fig. 1. Relative density of Fe/MgO: (a) green compacts, (b) sintered composites.

3.2. Resistivity

Results of the specific resistivity measurement confirm different effectiveness of MgO nanoparticles to create continuous dielectric coating on Fe microparticles in dependence on MgO particle size. In Fig. 2a it is shown that the most effective is MgO size of 30 nm. Specific resistivity of green compact rapidly increase with increasing content of MgO 30 nm particles in cold pressed composite. The smallest MgO 10 nm particles form significantly less effective dielectric network in comparison to green compact based on MgO 30 nm, because the formation of Fe–Fe interparticle connections is significant. Tendency curve of the resistivity of MgO 1000 nm particles based

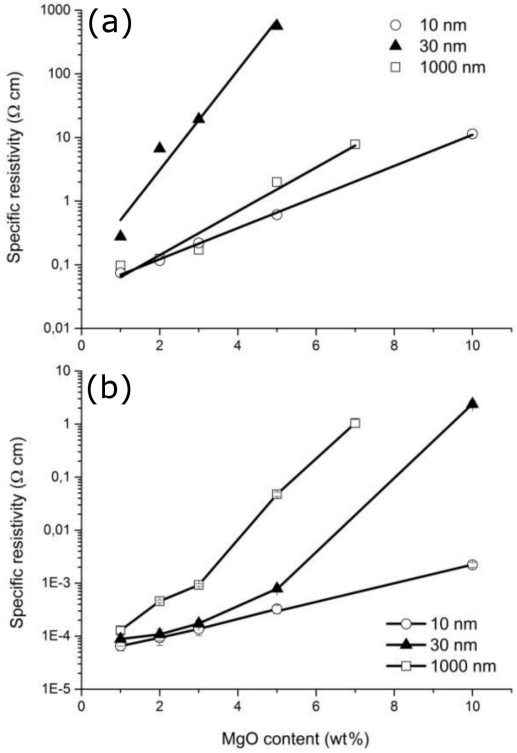

Fig. 2. Specific resistivity of Fe/MgO: (a) green compacts, (b) sintered composites.

composite is close to the curve of MgO 10 nm. Sintering process leads to decrease of the resistivity values of all experimental composites as it is shown in Fig. 2b. Good level of resistivity values are preserved in MgO 30 nm based composites, but resistivity of MgO 1000 nm composites are significantly higher after sintering. It is assumed to be caused by higher porosity probably arising among 1000 nm MgO particles. Analysis of the green and sintered resistivity of experimental composites confirms changes in densification processes. Evaluation based on density and specific resistivity could lead to preliminary result that the most suitable size of MgO particles is nearly size of 1 μm.

3.3. Magnetic properties

Analyses of the magnetic properties change show on functional properties of prepared Fe/xMgO composites. In Fig. 3 the coercive field in dependence on MgO content for different MgO particle size is shown. Composite based on MgO 30 nm particles provides the lowest coercive field values of green and sintered composite. In green compact, coercive field value reflects a level of residual stresses after cold pressing. Residual stresses could be relieved in sintering process above relaxation temperature. Sintering temperature 600 °C is enough to relieve residual stresses in iron. Coercive field decreased after sintering as it is shown in Fig. 3b. Increased coercive field values at higher content of MgO were observed. This phenomenon is dependent on the size of MgO particles. MgO 1000 nm particles in the composite leads to more rapid increasing of coercive field in comparison to smaller MgO 30 nm particles. Increasing coercive field is probably caused by thermal stresses due to different thermal expansion coefficient of MgO and Fe. Different MgO particle size creates different MgO phase distribution in the composite. It can be expected that thermal stresses are more significant in case of irregular distribution of MgO in the composite. Coercive field can be considered as an indicator of MgO agglomeration in the composite.

In Fig. 4 the real part of complex permeability at frequency 1 kHz (Fig. 4a) and 1 MHz (Fig. 4b) is plotted as a function of MgO insulation content in sintered composite material, for three particle sizes of MgO nanopowder.

In case of SMCs the real part of complex permeability at frequency 1 kHz is equal to the static initial permeability [4] and was found to be decreasing with the increase of MgO content for all MgO particle sizes, as expected. It is mainly due to the increasing inner demagnetizing fields arising from the surface magnetic poles on the iron particles insulated from each other [4–6], as the used ferromagnetic material and preparation process was the same and samples differed mainly in the insulation part (the content and particle size of MgO, as well as MgO distribution and porosity within composite). The higher the non-ferromagnetic content in SMC (insulation and pores), the larger the spaces between ferromagnetic particles causing the cut-off of the magnetic flux through

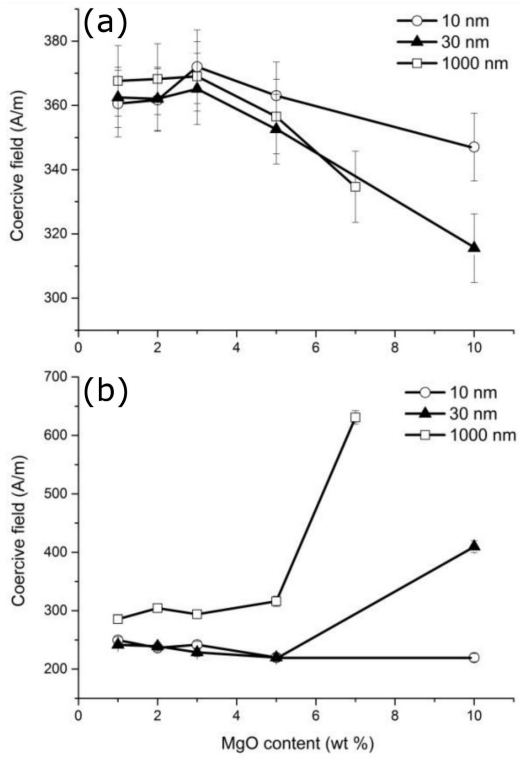

Fig. 3. Coercive field of Fe/MgO: (a) green compacts, (b) sintered composites.

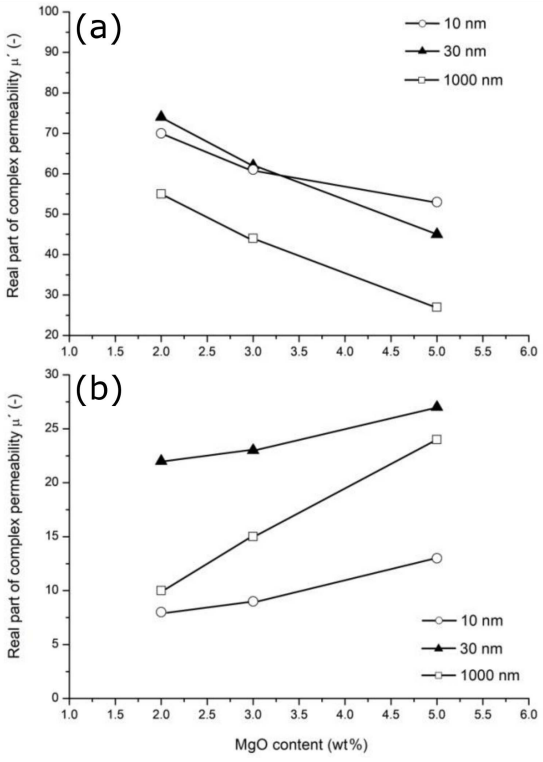

Fig. 4. Real part of complex permeability of sintered Fe/MgO composites at frequency (a) 1 kHz, (b) 1 MHz, for 10, 30, and 1000 nm MgO particle size.

SMC and lowering the magnetic interaction between iron particles. Finally it reflects in lower number of movable domain walls in material and hence lower value of permeability [4, 5].

Magnetic permeability is in general negatively influenced also by various defects in ferromagnetic material as dislocations, inclusions or voids, grain boundaries and internal stresses, all hindering the domain wall motion [5, 8].

On the other hand, the tendency of the real part of complex permeability at frequency 1 MHz is opposite, it is increasing with the increase of insulation content for all MgO particle sizes. The higher is the insulation content in SMC, the higher is the stability of the real part permeability to higher frequencies, due to the higher specific electrical resistivity of such SMC (the resonant frequency at which the real part permeability drops to its half value is proportional to the specific resistivity of material [9]). The specific resistivity of sintered samples is in Fig. 2b — it is increasing with the increase of MgO content as expected, but furthermore we can observe the higher resistivities for 30 nm and 1000 nm MgO particle sizes compared to the 10 nm MgO. The electrical resistivity of SMC depends on the quality of insulation of every ferromagnetic particle from each other, hence we can conclude the insulation of 10 nm MgO powder is the least effective one compared to 30 nm and 1000 nm, as 10 nm MgO particles are probably too small to create a layer completely covering iron particles and preventing electrical contacts between them. That is why in Fig. 4b the permeability dependence for 10 nm MgO is of the lowest values. The 1000 nm MgO powder particles conversely seem to be too large, causing the increase of porosity within SMC (reflected by the drop in real part permeability, Fig. 4a).

The most stable material for higher frequencies was found to be the SMC with 30 nm MgO insulation (the highest permeability at 1 MHz, Fig. 4b), with concurrently the highest static permeability (Fig. 4a), concluding that the 30 nm MgO particle sizes create the most effective insulation for iron-based composites.

3.4. Microstructure

Microstructure of the sintered Fe/MgO composites consists from origin iron particles divided by more or less continuous MgO network. Secondary phase of the composite is based on sintered MgO as it is shown in Fig. 5 (EDS line analysis). After sintering in air atmosphere, interphase Fe–MgO can contain Fe_3O_4 or non-stoichiometric $MgFe_2O_4$ — Table I (EDS point analysis) [10, 11]. Distribution of the dielectric secondary phase has crucial influence on functional properties of the soft magnetic composite. SEM backscatter electrons (BSE) technique was used to obtain contrast between heavy Fe (light in BSE image) and light Mg and O elements (dark regions in BSE).

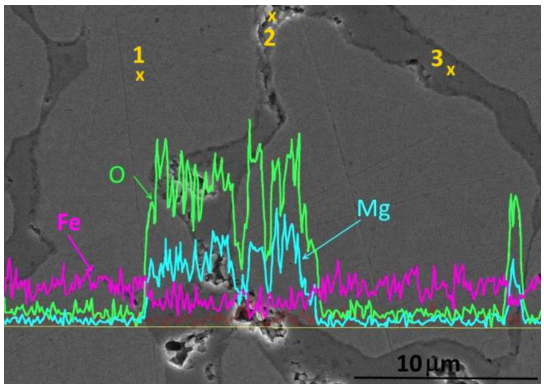

Fig. 5. Sintered Fe/2MgO composite, SEM EDS line analysis of Fe/MgO 30 nm interface.

TABLE I

EDS point analysis of Fe/MgO 30 nm interface

EDX analysis [wt%]	Fe	Mg	O
1	100	–	–
2	60.48	14.36	25.16
3	66.05	10.27	23.67

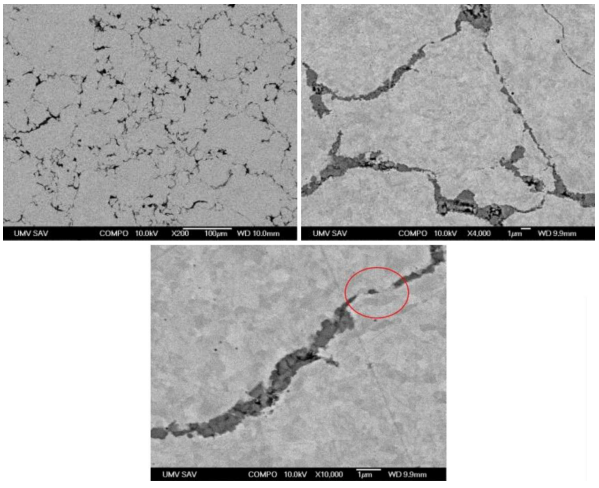

Fig. 6. Microstructure of Fe/2MgO 10 nm composite, SEM backscattering.

In Fig. 6 the microstructure of Fe/2MgO(10 nm) composite is shown. Minimal thickness of the dielectric layer is limited by MgO particle size. Small MgO 10 nm particles cover the iron microparticle by very thin layer, which follow all surface features of origin iron particles. Surface roughness of the iron microparticles and small MgO 10 nm particles lead to breaking of MgO layer. Iron–iron short bridges are created in the sintering process as it is documented in Fig. 6 — red marked detail. This Fe–Fe connections decrease the resistivity, but density of the composite is increased by sintering process.

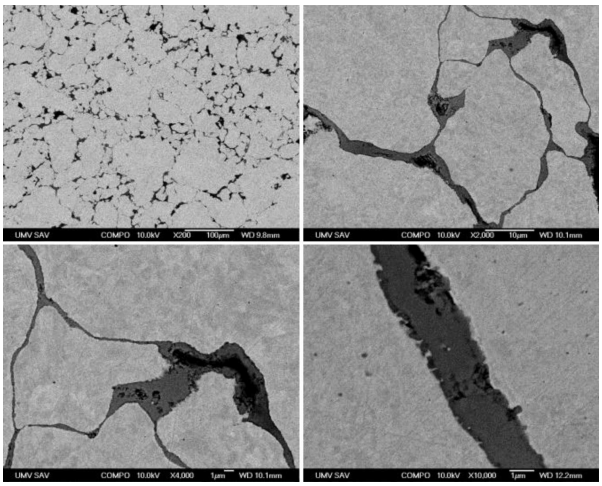

Fig. 7. Microstructure of Fe/2MgO 30 nm composite, SEM backscattering.

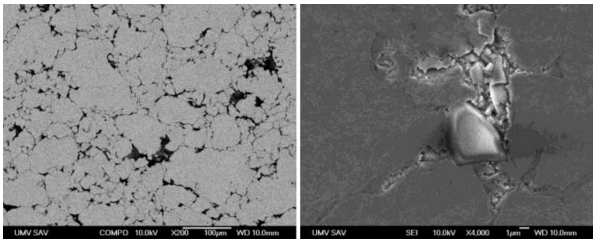

Fig. 8. Microstructure of Fe/2MgO(1000 nm) composite, SEM backscattering.

In case of Fe/MgO 30 nm composite in Fig. 7 it is possible to observe continuous MgO network. MgO nanoparticles of size 10 nm create effective barrier to creation of Fe-Fe bridges during the sintering, while thickness of the MgO layer is from 1 to 2 μm at content of 2 wt% MgO. Porosity is located to small pores in the interfaces of the composite.

Relatively regular distribution of the MgO in the composite is damaged if large MgO 1000 nm particles are applied in the composite as it is shown in Fig. 8. Large cubic MgO particles are pin up on the surface of iron particles in mixing process. Cold pressing imprint rigid MgO 1000 nm particles to iron particles, while Fe particle is deformed. Microstructure of the composite is recovered, residual stresses are relieved in sintering process. Large MgO 1000 nm particles avoid to create Fe–Fe connections, causing decreased density of the composite.

Identified densification mechanism of the Fe/MgO composite for different size of MgO particles is schematically depicted in Fig. 9. Application of these densification mechanism and microstructure development can be expected in case of the micro–nano powder systems based on microparticles with ability to plastic deformation and rigid nanoparticles. Specific densification mechanism together with secondary phase content ratio are the driving

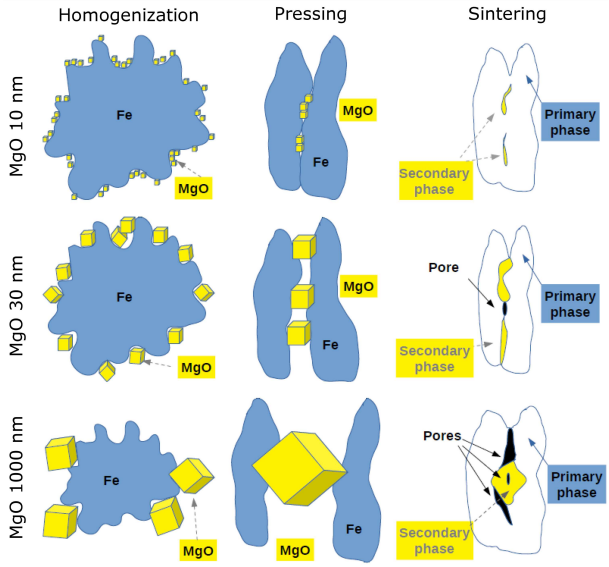

Fig. 9. Microstructure evolution mechanism of micro-nano powder composite based on different particle size of secondary constituent.

force for significant modification of the functional properties, as well as the mechanical properties of soft magnetic composite, as it is discussed in other work [11, 12].

4. Conclusions

Hierarchic micro-nano composite Fe/xMgO (where x is 1, 2, 3, 5, 7, and 10 wt%) was prepared by press and sinter method. Particle size of the secondary dielectric MgO nanophase significantly influences the densification process as well as the quality of insulation of each Fe microparticle from the others, hence the final properties of composite. Densification process of Fe–MgO powder mixture is well supported by 10 nm MgO particles. Specific resistivity increases with increasing MgO particle size, but distribution of the dielectric phase as well as size and shape distribution of the pores are different. Continuous MgO network creates effective barrier to creation of iron–iron bridges during the sintering in case of Fe/MgO composite based on 30 nm MgO particles. Fe/3MgO 30 nm composite was found to be the material with suitable distribution of MgO to create iron based soft magnetic composite stable for higher frequencies, supported by the magnetic properties analyses — the coercive field and the real part of complex permeability.

Acknowledgments

This work was supported by the Slovak Research and Development Agency under Grant APVV 0115-15 and the Scientific Grant Agency of the Ministry of Education, Science, Research and Sports and Slovak Academy of Sciences under Grant VEGA 2/0108/18.

References

[1] K.H.J. Buschow, *Concise Encyclopedia of Magnetic and Superconducting Materials*, Elsevier, Oxford 2005, eBook.

[2] K.J. Sunday, M.L. Taheri, *Metal Powder Rep.* **72**, 425 (2017).

[3] B. Ślusarek, B. Jankowski, K. Sokalski, J. Szczygłowski, *J. Alloys Comp.* **581**, 699 (2013).

[4] E.A. Périgo, B. Weidenfeller, P. Kollár, J. Füzer, *Appl. Phys. Rev.* **5**, 031301 (2018).

[5] E. Kneller, *Ferromagnetismus*, Springer, Berlin 1962.

[6] J.-L. Mattei, M. Le Floc'h, *J. Magn. Magn. Mater.* **257**, 335 (2003).

[7] L.J. Huang, L. Geng, H-X. Peng, *Prog. Mater. Sci.* **71**, 93 (2015).

[8] S. Chikazumi, *Physics of Ferromagnetism*, 2nd ed., Oxford University Press, New York 1999, eBook.

[9] F. Mazaleyrat, L.K. Varga, *J. Magn. Magn. Mater.* **215-216**, 253 (2000).

[10] N.M. Deraz, O.H. Abd-Elkader, *Int. J. Electrochem. Sci.* 8, 8632 (2013).

[11] R. Bureš, M. Fáberová, P. Kollár, J. Füzer, S. Dobák, F. Onderko, P. Kurek, *Acta Phys. Pol. A* **131**, 780 (2017).

[12] R. Bureš, M. Fáberová, P. Kurek, *Powder Metall. Progr.* **18**, 103 (2018).